Membrane Dynamics of the Water Transport Protein Aquaporin-1 in Intact Human Red Cells

Michael R. Cho,* David W. Knowles,# Barbara L. Smith,¶ John J. Moulds,§ Peter Agre,¶ Narla Mohandas,# and David E. Golan*

*Departments of Biological Chemistry and Molecular Pharmacology and of Medicine, Harvard Medical School, Hematology Division, Brigham and Women's Hospital, Boston, Massachusetts 02115; #Life Sciences Division, Lawrence Berkeley National Laboratory, University of California, Berkeley, California 94720; §Gamma Biologicals, Houston, Texas 77092; and ¶Departments of Biological Chemistry and Medicine, Johns Hopkins University School of Medicine, Baltimore, Maryland 21205 USA

ABSTRACT Aquaporin-1 (AQP1) is the prototype integral membrane protein water channel. Although the three-dimensional structure and water transport function of the molecule have been described, the physical interactions between AQP1 and other membrane components have not been characterized. Using fluorescein isothiocyanate–anti-Co3 (FITC-anti-Co3), a reagent specific for an extracellular epitope on AQP1, the fluorescence photobleaching recovery (FPR) and fluorescence imaged microdeformation (FIMD) techniques were performed on intact human red cells. By FPR, the fractional mobility of fluorescently labeled AQP1 (F-αAQP1) in the undeformed red cell membrane is 66 $\pm$ 10% and the average lateral diffusion coefficient is (3.1 $\pm$ 0.5) $\times$ 10^{-11} cm^2/s. F-αAQP1 fractional mobility is not significantly affected by antibody-induced immobilization of the major integral proteins band 3 or glycophorin A, indicating that AQP1 does not exist as a complex with these proteins. FIMD uses pipette aspiration of individual red cells to create a constant but reversible skeletal density gradient. F-αAQP1 distribution, like that of lipid-anchored proteins, is not at equilibrium after microdeformation. Over time, ~50% of the aspirated F-αAQP1 molecules migrate toward the membrane portion that had been maximally dilated, the aspirated cap. Based on the kinetics of migration, the F-αAQP1 lateral diffusion coefficient in the membrane projection is estimated to be 6×10^{-10} cm^2/s. These results suggest that AQP1 lateral mobility is regulated in the unperturbed membrane by passive steric hindrance imposed by the spectrin-based membrane skeleton and/or by skeleton-linked membrane components, and that release of these constraints by dilatation of the skeleton allows AQP1 to diffuse much more rapidly in the plane of the membrane.

INTRODUCTION

The red cell membrane is the structure upon which most models of the plasma membrane are based. Human red cells have provided the first examples of the function of important membrane skeletal proteins, including spectrin, ankyrin (ANK1), and protein 4.1, as well as important membrane transport proteins such as the band 3 anion exchanger (AE1), the glucose transporter (GLUT1), and the aquaporin water transport protein (AQP1). Red cell membranes have also proved to be remarkable subjects for clinical and basic studies. Pathological defects have been found to result from mutations in genes encoding several red cell membrane proteins (Lux and Palek, 1995), and physical analysis of red cell membranes has revealed detailed information about the functions of these proteins (Golan, 1989; Corbett et al., 1994a; Mohandas and Evans, 1994).

Although critical features of the structure and function of the AQP1 protein have been elucidated, little direct information exists regarding possible associations of AQP1 with other proteins. AQP1 is permeable to water but not to other solutes or charged molecules, including protons (Zeidel et al., 1992). In the membrane AQP1 is a homotetramer, with each subunit bearing an individual water channel (Jung et al., 1994) and each human red cell containing 40,000–50,000 tetramers (Smith and Agre, 1991). As first proposed by Jung et al. (1994), each subunit apparently comprises six bilayer-spanning α-helices surrounding a central structure termed the "hourglass," which is formed from the juxtaposition within the lipid bilayer of loop B (cytoplasmic leaflet) and loop E (exoplasmic leaflet) (Fig. 1). The extracellular loop (A) connecting the first and second bilayer-spanning domains contains the Ala/Val polymorphism at residue 45 that is responsible for the Colton blood group antigens Co^a and Co^b (Preston et al., 1994; Smith et al., 1994). The three-dimensional shape of the protein is becoming defined to nearly atomic levels of resolution (Cheng et al., 1997; Li et al., 1997; Walz et al., 1997). The N-terminus (~15 aa) and C-terminus (~36 aa) reside in the cytoplasm, but it is not known whether these domains interact with other proteins.

Several indirect observations suggest that aquaporins may associate with other proteins in differentiated tissues, either while undergoing membrane sorting during cellular biogenesis or as a response to specific stimuli. AQP1 was initially thought to be linked to the red cell membrane skeleton, because it pellets with the spectrin-actin matrix in low concentrations of Triton X-100 (Denker et al., 1988), but the protein was later shown to be solubilized in higher concentrations of the detergent (Smith and Agre, 1991).

Received for publication 13 July 1998 and in final form 14 October 1998.

Address reprint requests to Dr. David E. Golan, Department of Biological Chemistry and Molecular Pharmacology, Harvard Medical School, 250 Longwood Avenue, Boston, MA 02115. Tel.: 617-432-2256; Fax: 617-432-3833; E-mail: degolan@warren.med.harvard.edu.

Drs. Cho and Knowles contributed equally to this work.

0006-3495/99/02/1136/09 $2.00

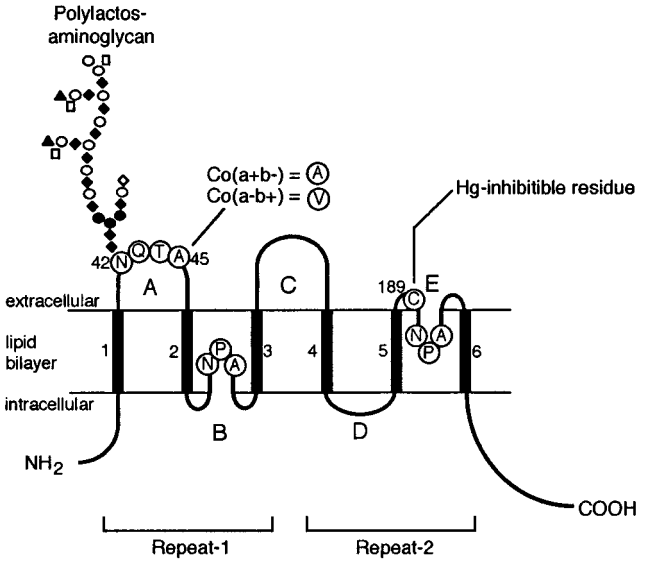

FIGURE 1 Schematic diagram representing the structure of a monomeric subunit of the AQP1 water transport protein.

Although in most tissues AQP1 is expressed in apical and basolateral membranes, AQP1 is sorted only to the apical membrane in choroid plexus (Nielsen et al., 1997). Other aquaporins also exhibit highly specific membrane targeting—AQP3 and AQP4 reside in basolateral membranes (Frigeri et al., 1995; Ecelbarger et al., 1995; Terris et al., 1995), and AQP5 is present exclusively in apical membranes (Nielsen et al., 1997). In proximal renal tubules, colchicine disruption of microtubules leads to a block in endocytosis and to redistribution of AQP1 from the plasma membrane to intracellular vesicles (Elkjaer et al., 1995). In contrast, secretin appears to induce the redistribution of AQP1 from intracellular vesicles to the plasma membrane of cholangiocytes (Marinelli et al., 1997). Within the renal collecting duct, vasopressin stimulation of principal cells produces a major redistribution of the AQP2 protein from intracellular vesicles to the plasma membrane (Nielsen et al., 1993).

Physical methods can be used to measure the lateral redistribution of fluorescently labeled red cell membrane proteins. Laser-induced photobleaching of red cell membranes has permitted determinations of the rates of lateral diffusion and the magnitudes of the immobile fraction of glycophorins and band 3 (Golan and Veatch, 1980; Golan, 1989; Corbett and Golan, 1993; Corbett et al., 1994a). These studies have identified a role for the membrane skeleton in restricting lateral diffusion of certain integral membrane proteins. Micropipette aspiration of red cell membranes produces extended membrane projections in which the membrane skeletal protein density exhibits a gradient along the aspirated projection (Discher et al., 1994, 1995; Discher and Mohandas, 1996; Knowles et al., 1997). By using this technique, the role of the membrane skeleton in regulating redistribution of specific membrane components can be quantitatively assessed by kinetic measurements of fluorescently imaged red cell membranes.

In this report we have affinity-purified and fluorescently labeled IgG specific for the Colton Co3 antigen determinant on the surface of the AQP1 polypeptide and have used this reagent to determine the lateral mobility of fluorescently labeled AQP1 (F-αAQP1) in intact red cell membranes by measuring the diffusion and redistribution of F-αAQP1 in unperturbed red cells and in aspirated membrane projections. Our studies identify unique and unexpected characteristics of F-αAQP1 mobility, suggesting that AQP1 is not linked directly to either the membrane skeleton or to skeleton-linked membrane components, but that lateral diffusion of the protein is nonetheless retarded in unperturbed cells by passive steric hindrance within the membrane imposed by skeleton-associated components.

MATERIALS AND METHODS

Purification and fluorescent conjugation of anti-Co3 antibodies

Extremely rare individuals lack Colton antigens and develop high-titer antibodies to Co3 that are reactive with red cells carrying Co^a or Co^b antigens. Placental extract was prepared from a woman (blood type O, Rh positive, Co null) who had developed anti-Co3 IgG during pregnancy (Moulds et al., 1978; Lacey et al., 1987). The extract was initially purified by sequential ammonium sulfate precipitation. After precipitation of other proteins in 30% saturated ammonium sulfate, anti-Co3 was precipitated in 50% saturated ammonium sulfate, resolubilized in 7.5 mM Na phosphate, 150 mM NaCl, pH 7.4 (phosphate-buffered saline, PBS), and further processed at 4°C. After centrifugation at 3000 $\times$ g for 20 min, the supernatant was loaded onto a protein G-sepharose 4 fast flow column (Pharmacia, Piscataway, NJ) preequilibrated with PBS, washed with PBS, eluted with 1 M acetic acid, and neutralized with 1 M Tris. Peak protein fractions were concentrated using polyethylene glycol and dialyzed against PBS. The concentrate was diluted 12-fold with 150 mM NaCl, 50 mM Na_2CO_3, pH 9.0, to a concentration of 6 mg IgG/ml, and 1.8 ml of the resulting material was labeled with fluorescein isothiocyanate (FITC) by the method of Stolpen et al. (1988). Unreacted FITC was removed by passing the material over a Sephadex G-25M PD-10 gel filtration column (Pharmacia) preequilibrated with PBS at room temperature. Peak protein fractions and FITC content were determined by measuring the optical density at 280 and at 495 nm, and NaN_3 was added to 1 mM final concentration.

FITC-labeled anti-Co3 IgG was further purified by adsorption and elution from group O, Co:3 red cells. Antibodies were mixed with 4 ml of washed red cells and incubated for 1 h at 37°C and overnight at 4°C. The cells were then washed in PBS, and membranes were prepared as described (Bennett, 1983), washed in PBS, and resuspended to 6 ml with PBS. Ether elution was then performed by adding an equal volume of diethyl ether to the sample, mixing, and incubating at 37°C for 30 min (Rubin, 1963). After centrifugation at 1500 $\times$ g at room temperature for 10 min, the hemoglobin-free eluate (6 ml) was recovered. After an additional 15-min incubation at 37°C to evaporate residual ether, the eluate was concentrated to 0.4 ml by ultrafiltration, NaN_3 was added to 1 mM final concentration, and the FITC-anti-Co3 IgG was stored in the dark at 4°C.

Fluorescent labeling of AQP1

Blood was washed twice in PBS and once in PBS containing 10% fetal bovine serum (FBS). About 100 μl of packed red cells was incubated in 10% FBS/PBS for 15 min at room temperature to block nonspecific

binding. Two microliters of packed red cells were then incubated with 8 μl of FITC-conjugated anti-Co3 antibodies for 45 min at room temperature, with gentle shaking. Cells were then washed three times in PBS.

Although the use of bivalent anti-Co3 IgG to label AQP1 could have theoretically resulted in cross-linking of AQP1 monomers on the membrane, this was very unlikely to affect the results of lateral mobility and microdeformation experiments on AQP1 in intact red cells. The most favored cross-linking of AQP1 monomers by IgG would involve two closely apposed monomers in the AQP1 homotetramer complex, which would be expected to undergo lateral movement as a single unit in the plane of the membrane.

Fluorescent labeling of band 3

Blood was washed three times in high-potassium PBS (KPBS) (140 mM KCl, 15 mM $NaPO_4$, 10 mM glucose, pH 7.4). Band 3 was labeled by incubating 100 μl of packed red cells with 40 μl of eosin-5-maleimide (EMA) (0.25 mg/ml in KPBS; Molecular Probes, Eugene, OR) for 12 min at room temperature. After incubation cells were washed extensively in KPBS with 1% BSA. Under these conditions >90% of the membrane-associated fluorescence was covalently bound to band 3 (Corbett and Golan, 1993; Corbett et al., 1994a; unpublished observations).

Fluorescent labeling of actin

Cytoskeletal actin was labeled using rhodamine phalloidin and a technique modified from Discher and Mohandas (1996). Briefly, 5 μl of washed, packed red cells were lysed in 20 μl of 20 mOsm PBS with 1 mM Mg-ATP and 4 μl of rhodamine phalloidin (Molecular Probes). Cells were incubated for 15 min at 0°C, resealed by adding 2.5 μl of 3000 mOsm PBS, and further incubated for 30 min at 37°C. The resealed cells, which had 20% of the normal hemoglobin content, showed normal morphology and mechanical properties (Discher and Mohandas, 1996).

Antibody incubation

Washed red cells in 10% suspension were incubated with 20 μg/ml (final concentration) of anti-band 3 monoclonal antibody (mAb) (Brac 18) or 80 μg/ml (final concentration) of anti-glycophorin A mAb (R10) for 45 min at room temperature. These treatments caused complete lateral immobilization of band 3 or glycophorin A, respectively (Knowles et al., 1994; the present study).

Lateral mobility measurements

Fluorescence photobleaching recovery (FPR) (Axelrod et al., 1979) was used to measure F-αAQP1 and band 3 lateral mobility in the membranes of intact red cells. Briefly, the 488-nm line from an argon ion laser of Gaussian spatial profile was selected and focused onto a microscope stage. A short (typically 100 ms) intense (typically 1 mW) laser pulse was used to photobleach a spot of 0.7 μm radius on the upper membrane of a single red cell. The fluorescence intensity of the bleached spot was then monitored by using periodic low-intensity (typically 0.1 μW) laser pulses. Fluorescence recovery resulted from the lateral diffusion of unbleached fluorophores into the bleached area. A nonlinear least-squares fitting procedure (Bevington, 1969) was used to determine the lateral diffusion coefficient (D) and fractional mobility (f) of F-αAQP1 and band 3 from the fluorescence recovery data. Details of the optics and electronics of our apparatus have been described (Corbett and Golan, 1993). All lateral mobility measurements were performed at 37°C. The local temperature rise caused by laser-induced heating of surface fluorophores during the bleaching pulse was calculated to be < 0.02°C, and that caused by heating of intracellular hemoglobin to be 0.03°C (Corbett et al., 1994b).

Microdeformation measurements

Fluorescence imaged microdeformation (FIMD) was used to quantify redistribution of F-αAQP1 and other membrane components after micropipette aspiration (Discher et al., 1994). Briefly, the membrane protein of interest was fluorescently labeled, and a single fluorescently labeled red cell was partially aspirated into a glass micropipette with an internal diameter between 1 and 1.5 μm. Aspiration created an in-plane deformation of the membrane skeleton, which condensed to enter the micropipette and subsequently dilated down the micropipette. Aspiration length scaled by the micropipette radius (L/R_p) was predetermined by the surface-to-volume ratio of the cell (osmotically controlled) and by the large compressibility modulus of the lipid bilayer. The typical aspiration length was ~8 μm. The relative density of a fluorescently labeled component at different locations along the aspiration length was quantified as the fluorescence intensity at that location normalized by the fluorescence intensity of the fluorescently labeled molecules in the spherical portion of the aspirated cell.

RESULTS

A large fraction of F-αAQP1 is laterally mobile in membranes of intact red cells

AQP1, labeled with FITC-conjugated anti-Co3 antibodies, was found to be uniformly distributed on the normal red cell surface (Fig. 2). This surface distribution pattern was similar to that of other integral red cell membrane proteins (Golan, 1989). By fluorescence video microscopy, FITC-conjugated anti-Co3 antibodies failed to label Colton-null red cells that were deficient in AQP1 (images not shown), confirming the specificity of the antibody. FPR was used to quantify the lateral mobility of specifically labeled F-αAQP1 in membranes of intact normal red cells. A large fraction of F-αAQP1 (66 $\pm$ 10%) was laterally mobile in these membranes, and the average lateral diffusion coeffi-

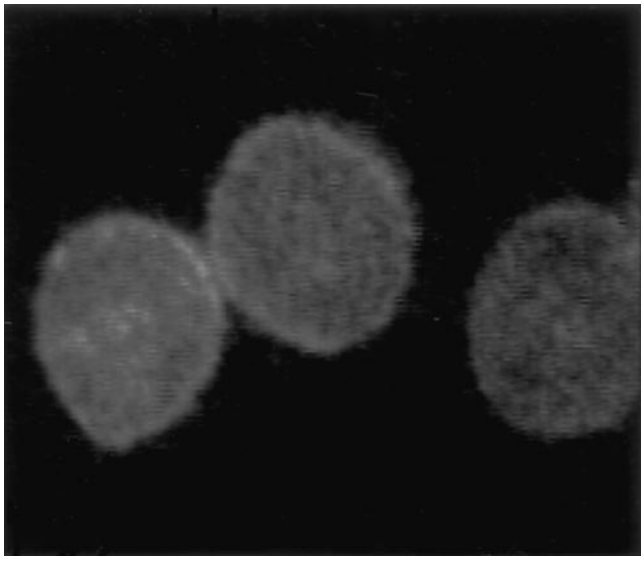

FIGURE 2 Cell surface distribution of FITC-conjugated anti-Co3 (anti-AQP1) antibodies. Red cells were observed with a Zeiss Axioskop microscope and a 100×/1.3 NA objective at room temperature. Fluorescence images were recorded, background subtracted, and frame averaged with an image processor (Image-1; Universal Imaging, West Chester, PA).

cient was (3.1 ± 0.5) × 10^{-11} cm^2/s (Fig. 3 and Table 1). The similarity between this diffusivity and that of band 3 and glycophorin A, the two major integral membrane proteins of human red cells (Golan and Veatch, 1980; Golan, 1989; Corbett and Golan, 1993; Corbett et al., 1994a), suggested that AQP1 lateral diffusion could be regulated by steric interactions similar to those that retard band 3 and glycophorin A diffusion.

Although AQP1-deficient red cells exhibit a marked reduction in water permeability, it is not known whether the protein contributes to the integrity of the red cell membrane. The lateral mobility of band 3 was measured in Colton-null red cells as a probe for membrane bilayer and membrane skeletal integrity, because band 3 mobility has been shown to be sensitive to changes in red cell membrane protein and lipid content and organization (Corbett and Golan, 1993; Corbett et al., 1994a; Jarolim et al., 1994; Liu et al., 1995; Golan et al., 1996). As shown in Table 2, the lateral mobility of band 3 in Colton-null red cells did not differ from that in normal red cells. In addition, Colton-null red cells exhibited the biconcave disc morphology characteristic of normal red cells. These data were consistent with the interpretation that AQP1 expression is not required for structural integrity of the red cell membrane bilayer and the spectrin-based membrane skeleton.

Multiple studies have indicated that integral membrane proteins such as band 3, glycophorin A, and glycophorin C interact with the normal membrane skeleton. Increased interaction is found in some pathologic red cells (Liu et al., 1990; Corbett and Golan, 1993; Liu et al., 1995), and increased interaction can be induced in normal red cells by anti-band 3 and anti-glycophorin A antibodies (Chasis et al., 1985, 1988; Knowles et al., 1994). To examine the possibility that band 3 or glycophorin A exists in a complex with AQP1 in the normal red cell membrane, the lateral mobility of F-αAQP1 was quantified after antibody-induced lateral immobilization of band 3 or glycophorin A. Consistent with previous reports (Nash and Gratzer, 1993), band 3 was found to be completely immobilized by incubation of normal red cells with anti-band 3 mAb (Brac 18) at a final concentration of 20 μg/ml. Band 3 immobilization was also induced by incubating red cells with anti-glycophorin A mAb (R10) at a final concentration of 80 μg/ml, consistent with previous studies (Knowles et al., 1994). Neither Brac 18 nor R10 treatment of normal red cells induced lateral immobilization of F-αAQP1, however. Brac 18 caused the F-αAQP1 lateral diffusion coefficent to decrease from 3.1 × 10^{-11} cm^2/s to 1.8 × 10^{-11} cm^2/s, and the fractional mobility to decrease from 66% to 50%. R10 caused the F-αAQP1 lateral diffusion coefficient and fractional mobility to decrease to 1.1 × 10^{-11} cm^2/s and 56%, respectively (Table 3). In contrast, cross-linking of FITC-conjugated anti-Co3 IgG by anti-human IgG caused complete lateral immobilization of F-αAQP1 on normal red cells (fractional mobility, 3 ± 2%), without morphologic F-αAQP1 capping by fluorescence video microscopy (not shown). These data suggested that AQP1 does not exist in a complex with either band 3 or glycophorin A in the normal red cell membrane.

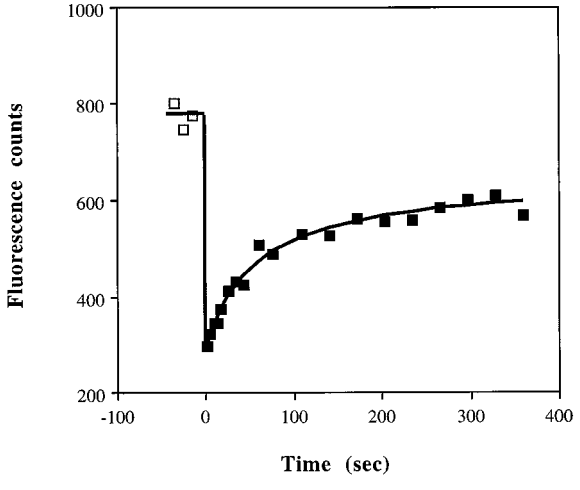

FIGURE 3 Representative FPR curve depicting the lateral mobility of AQP1 in an intact red cell. Each data point represents the average of three fluorescence measurements before (□) or after (■) a brief bleaching laser pulse. The experiment was performed at 37°C. Diffusion coefficient, 2.5 × 10^{-11} cm^2/s; fractional mobility, 64%.

TABLE 1 AQP1 lateral mobility in Colton-null and normal red cells

Sample	D (× 10^{11} cm^2/s)	f (%)
Colton-null	*	*
Control 1	2.7 ± 1.8	52 ± 8
Control 2	2.5 ± 1.0	84 ± 7
Control 3	4.2 ± 2.1	61 ± 6

AQP1 lateral mobility was determined by FPR. Control samples consisted of normal group O, Co:3 red cells. Values represent mean ± SD from 8–14 independent experiments for each sample.
* Fluorescence video microscopy confirmed the lack of AQP1 expression on Colton-null red cells.

Microdeformation induces striking migration of F-αAQP1 toward the cap of the aspirated membrane projection

Imaging of protein density gradients after microdeformation of intact red cells has provided unique information concerning interactions between integral proteins and skeletal pro-

TABLE 2 Band 3 lateral mobility in Colton-null and normal red cells

Sample	D (× 10^{11} cm^2/s)	f (%)
Colton-null	1.4 ± 0.5	40 ± 6
Control 1	1.1 ± 0.4	58 ± 8
Control 2	1.5 ± 0.6	38 ± 5
Control 3	1.5 ± 0.7	41 ± 13

Band 3 lateral mobility was determined by FPR. Control samples consisted of normal group O, Co:3 red cells. Values represent mean ± SD from 8–14 independent experiments for each sample. Band 3 lateral mobility in Colton-null red cells was indistinguishable from that in control red cells.

TABLE 3 Effects of antibody treatments on AQP1 and band 3 lateral mobility in normal red cells

Condition	Band 3 D ($\times 10^{11}$ cm^2/s)	Band 3 f (%)	AQP1 D ($\times 10^{11}$ cm^2/s)	AQP1 f (%)
Brac 18 mAb	ND	6 ± 5	1.8 ± 0.7	50 ± 17
R10 mAb	ND	11 ± 5	1.1 ± 0.4	56 ± 14

Control red cells were incubated with Brac 18 (anti-band 3) or R10 (anti-glycophorin A) mAbs. Lateral mobility was determined by FPR. Values represent mean $\pm$ SD from 8–14 independent experiments for each condition. Both Brac 18 and R10 mAbs induced lateral immobilization of band 3. These same antibody treatments did not cause AQP1 immobilization, however.

ND, Diffusion coefficient cannot be accurately determined for $f < 20\%$.

teins in the intact red cell membrane (Discher et al., 1995; Discher and Mohandas, 1996). Here, novel FIMD techniques were used to examine dynamic changes in the distribution of F-αAQP1, membrane skeletal actin, and band 3 induced upon microdeformation. Consistent with previous reports, deformation induced a density gradient of skeletal actin labeled by rhodamine phalloidin, such that the relative actin density was highest at the pipette entrance and lowest at the aspirated cap (Fig. 4). The redistribution of actin density reached equilibrium rapidly during the deformation, which has been shown to be elastic for moderate aspiration lengths (Discher et al., 1994; Discher and Mohandas, 1996; Knowles et al., 1997). No further actin redistribution was observed at later times after cell deformation. EMA-labeled band 3 showed a density gradient that was similar to that of actin, except that the slope of the band 3 density gradient was less steep than that of the actin gradient. F-αAQP1 redistribution in response to microdeformation was distinctly different from that of actin and band 3 (Fig. 4). Immediately after deformation, the density gradient of F-αAQP1 was less steep than that of band 3 but steeper than that of a fluorescently labeled phospholipid (Knowles et al., 1997; data not shown). At long times after deformation ($>$15 min), a major fraction of F-αAQP1 was found to have migrated along the membrane projection toward the aspiration cap (Fig. 4). The kinetics of F-αAQP1 migration were estimated by quantifying the alteration in the F-αAQP1 density map with time (Fig. 5 *A*). Fluorescence images recorded immediately ($\sim$1 s) after cell deformation showed that the deformation process itself did not cause F-αAQP1 accumulation at the cap. With time after deformation, however, F-αAQP1 progressively migrated toward the cap until a steady state was reached. At steady state, it was estimated that 45–60% of the F-αAQP1 molecules in the aspirated membrane projection had migrated toward the cap.

These observations suggested that AQP1 in the aspirated projection was capable of rapid lateral diffusion toward membrane areas of increasing skeletal dilatation. To calculate a mean diffusivity for this process, a characteristic migration half-time of 100–200 s was estimated from a plot of cap mass fraction versus time (Fig. 5 *B*). By modeling the characteristic area for diffusion as the surface of an aspirated membrane cylinder, the diffusivity of F-αAQP1 in the

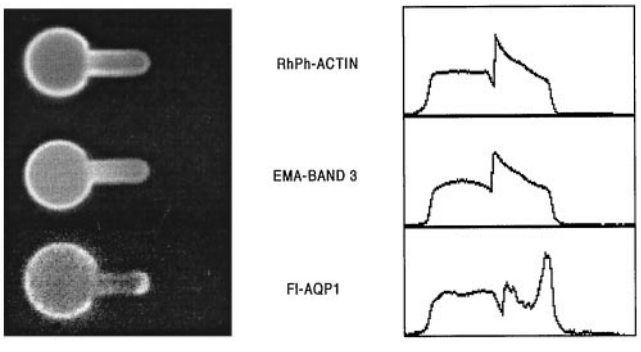

FIGURE 4 Fluorescence images of intensity gradients for actin, band 3, and AQP1 distributions after aspiration of the red cell membrane. The corresponding fluorescence intensity profiles are shown next to the fluorescence images. The fluorescence intensity was greatest at the entrance of the aspirated membrane and decreased monotonically along the projection for actin and band 3, whereas the highest intensity for AQP1 was found at the cap.

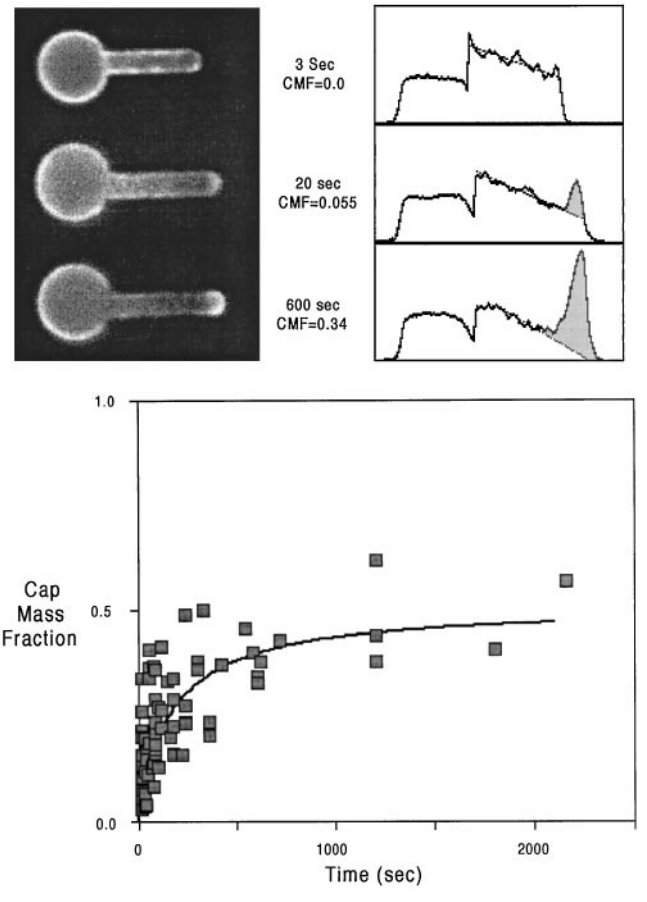

FIGURE 5 (*A*) Changes in the AQP1 fluorescence intensity distribution in the aspirated red cell membrane at three different times after microdeformation. The corresponding AQP1 fluorescence intensity profiles are shown next to the fluorescence images. The shaded areas indicate the calculated AQP1 cap mass fraction (CMF) that had migrated toward the cap. (*B*) Kinetics of AQP1 migration toward the cap after microdeformation. The fraction of AQP1 that had migrated toward the cap after microdeformation was calculated and plotted as a function of time. Data were fitted by eye.

membrane projection was estimated to be $4-8 \times 10^{-10}$ cm^2/s. This value is ~20-fold greater than the average F-αAQP1 lateral diffusion coefficient measured with the FPR technique, suggesting that there was a fraction of AQP1 molecules capable of diffusing much more rapidly than the average in the native (unperturbed) red cell membrane, and/or that such a population of molecules was created upon microdeformation of the membrane. Additional FPR experiments were performed to estimate the relative importance of these two possibilites. In these experiments, fluorescence recovery was followed at 0.5-s intervals for the first 10 s after photobleaching a spot on an anti-Co3 labeled undeformed red cell. As shown in Fig. 6, $12 \pm 3\%$ of F-αAQP1 molecules were capable of rapid lateral diffusion (diffusion coefficient $\sim 10^{-10}$ to 10^{-9} cm^2/s) during the first 10 s of measurement ($n = 10$ independent experiments). In contrast, similar FPR experiments showed that band 3 and glycophorins did not exhibit rapid lateral diffusion during the 10-s measurement period. Only $4 \pm 2\%$ of the band 3 label and $4 \pm 3\%$ of the glycophorin label recovered during the 10 s period, consistent with the recovery expected assuming that all molecules diffused at the average rate of $\sim 10^{-11}$ cm^2/s. Taken together, these data suggested that only a small fraction (5–10%) of AQP1 molecules were capable of rapid lateral diffusion in the native red cell membrane, and that dilatation of the membrane skeleton induced a significant increase in this fraction.

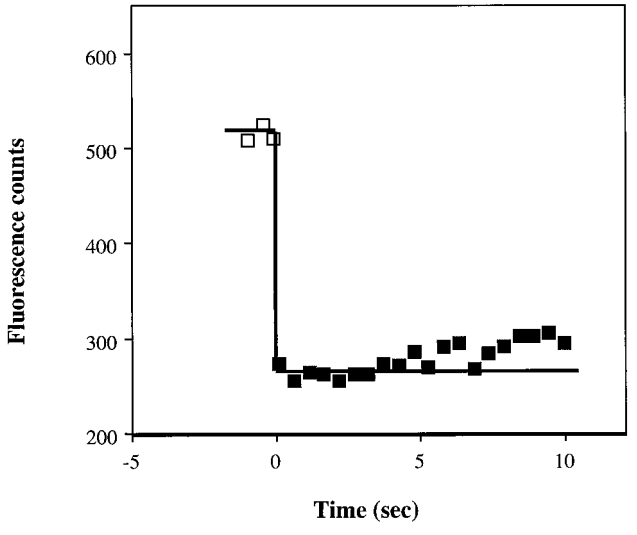

FIGURE 6 Representative FPR curve depicting the rapid mobility fraction of the laterally mobile AQP1 in an intact red cell. Each data point represents the average of three fluorescence measurements before (□) or after (■) a brief bleaching laser pulse. After the bleaching pulse, fluorescence counts were measured at 0.5-s intervals. The experiment was performed at 37°C. Recovery of fluorescence during the first 10 s indicated that a small but significant subpopulation of AQP1 molecules is capable of rapid lateral diffusion. Because the fitting routine used to analyze typical FPR curves could not be reliably used for analysis of the rapid mobility experiments, the fractional mobility was determined by calculating the ratio $(F(\infty) - F(0))/(F(-) - F(0))$, where $F(-)$ is the fluorescence counts before bleaching, $F(0)$ is the fluorescence counts immediately after bleaching, and $F(\infty)$ is the fluorescence counts at the end of the 10-s experiment. An approximate lateral diffusion coefficient of 10^{-10} to 10^{-9} cm^2/s was estimated by assuming that the characteristic half-time for the rapidly mobile AQP1 molecules is ~1–5 s. Fractional mobility, 10%.

DISCUSSION

We have used FPR and FIMD to characterize the constraints on AQP1 lateral mobility in unperturbed and aspirated membranes of intact human red cells. Fluorescence images show that AQP1 is uniformly distributed on the red cell surface. FPR indicates that, although AQP1 lateral mobility in the unperturbed membrane is similar to that of other integral proteins such as band 3 and glycophorin A, AQP1 does not exist as a complex with either of these integral proteins. FIMD demonstrates that the pattern of AQP1 redistribution in response to microdeformation does not resemble that of either actin or band 3. Rather, AQP1 behavior under microdeformation is similar to that of molecules such as CD59 that are not directly linked to the membrane skeleton. At least 50% of AQP1 molecules in the aspirated membrane projection are capable of diffusing toward the cap with a rate ~20-fold greater than that in the unperturbed membrane.

In intact red cell membranes, lipids and lipid-linked membrane proteins manifest lateral diffusion coefficients of $\sim 10^{-9}$ cm^2/s and fractional mobilities of 90–100%, whereas integral membrane proteins such as band 3 and glycophorin A have diffusion coefficients of $\sim 10^{-11}$ cm^2/s and fractional mobilities of 40–70% (Golan, 1989; Corbett and Golan, 1993; Corbett et al., 1994a). The AQP1 lateral diffusion rate is only twofold greater than that of band 3 (Table 1) and is comparable to that of glycophorin A (Golan, 1989). Similarly, the AQP1 fractional mobility of 66% is comparable to that of other integral proteins. These observations suggest that the lateral diffusion of AQP1 is constrained in unperturbed red cell membranes.

At least three mechanisms can be hypothesized to explain these constraints on AQP1 mobility. First, based on the findings that AQP1 lateral mobility is similar to that of band 3 and glycophorin A in the unperturbed red cell membrane, and that 34% of AQP1 molecules are laterally immobile on the FPR time scale (6 min), AQP1, like band 3 and glycophorin A, could interact directly with the red cell membrane skeleton. Although it has been suggested that AQP1 colocalizes with the caveolar scaffolding protein caveolin in endothelial cells (Schnitzer and Oh, 1996), no binding interactions between AQP1 and other proteins associated with the red cell membrane have been demonstrated. Moreover, the observation that AQP1 behaves like lipid-linked proteins in response to microdeformation provides strong evidence that AQP1 is not directly linked to the membrane skeleton.

Second, AQP1 lateral diffusion could be restricted by steric interactions between AQP1 and other integral proteins such as band 3. A theoretical model describing this mode of interaction has been developed by Minton (1989). One

important parameter in the model is the fraction of the red cell membrane surface (~150 μm^2) that is occupied by proteins. Based on the measured physical properties of AQP1 and band 3 (the major integral protein), AQP1 and band 3 are predicted to occupy ~3% (Agre et al., 1993) and ~17% (Golan et al., 1984) of the cell surface, respectively. The intramembranous portions of glycophorins and other integral proteins together are likely to occupy at most an additional 17% of the cell surface. Based on these approximations, the model predicts a reduction in the rate of AQP1 lateral diffusion, compared to that of AQP1 diffusing "freely" in a pure lipid bilayer, of ~50%. Thus, although steric interactions between AQP1 and other integral proteins could be partially responsible for the slowing of AQP1 diffusion in unperturbed red cells, these interactions are unlikely to explain completely the ~100-fold difference between the lateral diffusion rates of AQP1 and membrane lipids in the unperturbed membrane. Furthermore, the observation that band 3 or glycophorin A immobilization only slightly reduces the AQP1 lateral diffusion rate suggests that these immobilized complexes represent physical barriers that could only partially hinder the random diffusion of AQP1.

Third, AQP1 lateral mobility in the unperturbed membrane could be retarded by steric hindrance imposed by the spectrin-based membrane skeleton. Such interactions have been demonstrated to regulate the lateral mobility of other integral proteins, in that the rate of band 3 diffusion is inversely related to the spectrin content of intact human red cells. Studies on cells from patients with hereditary spherocytosis predict that band 3 and glycophorin A would diffuse laterally at a rate of 9×10^{-10} cm^2/s in the complete absence of a spectrin-based skeleton (Cho et al., 1999; Corbett et al., 1994a; unpublished observations). In the present work, the rate of AQP1 diffusion is increased by ~20-fold (to ~6×10^{-10} cm^2/s) as the membrane skeletal density is decreased in the aspirated membrane projection. This magnitude of increase is similar to that demonstrated for band 3 diffusion in aspirated membrane projections (Berk and Hochmuth, 1992), suggesting that steric hindrance imposed by the membrane skeleton could provide a plausible mechanism for AQP1 mobility restriction in the unperturbed membrane. Furthermore, this analysis suggests that AQP1 lateral mobility in the aspirated membrane approaches diffusion in the "idealized" spectrin-free environment, where diffusing molecules are restricted only by the viscosity of the lipid bilayer, and that microdeformation allows significantly faster AQP1 diffusion because this perturbation decreases passive mobility constraints imposed by the membrane skeleton.

Passive steric interactions, unlike direct binding interactions with membrane skeletal components, should not cause lateral immobilization of AQP1. By FPR, ~35% of AQP1 molecules appear to be immobile, however. This laterally immobile fraction could be accounted for by tight binding of a population of AQP1 molecules to the membrane skeleton, although biochemical studies have failed to elucidate such a binding partner for AQP1 in the red cell. We favor instead a model in which AQP1 is considered to undergo anomalous subdiffusion rather than either free diffusion or tight binding interactions (Feder et al., 1996). In the anomalous subdiffusion model, integral protein lateral mobility is assumed to be complete (i.e., there is no immobile fraction) but restricted by a dense polymer-like meshwork consisting of skeletally defined "corrals" or other obstacles to lateral diffusion. The integral protein therefore diffuses on a time scale that is much longer than that of the typical FPR experiment, resulting in an apparently immobile fraction on the FPR time scale. The anomalous subdiffusion model can only be considered if experimental FPR data are fitted equally well by the random diffusion and the anomalous subdiffusion models (Feder et al., 1996).

To test the hypothesis that the lateral mobility of AQP1 is governed by anomalous subdiffusion, we have reanalyzed our experimental AQP1 and band 3 fluorescence recovery data by using the anomalous subdiffusion model. As indicated by the quality of the fit (Fig. 7), AQP1 lateral mobility is described equally well by the anomalous subdiffusion and the random diffusion models (compare Figs. 3 and 7). The recovery half-time calculated assuming anomalous subdiffusion is 486 ± 222 s, and that calculated assuming random diffusion with an immobile fraction is 73 ± 33 s. This comparison suggests that complete AQP1 diffusion could be achieved on a time scale that is about an order of magnitude longer than the typical FPR experiment. Similar analyses of experimental band 3 fluorescence recovery data are not well described by the anomalous subdiffusion model (curve fits not shown). The latter finding is consistent with the interpretation that, because a fraction of band 3 binds tightly to ankyrin, band 3 does not diffuse completely, even on a much longer time scale. In contrast, our analysis

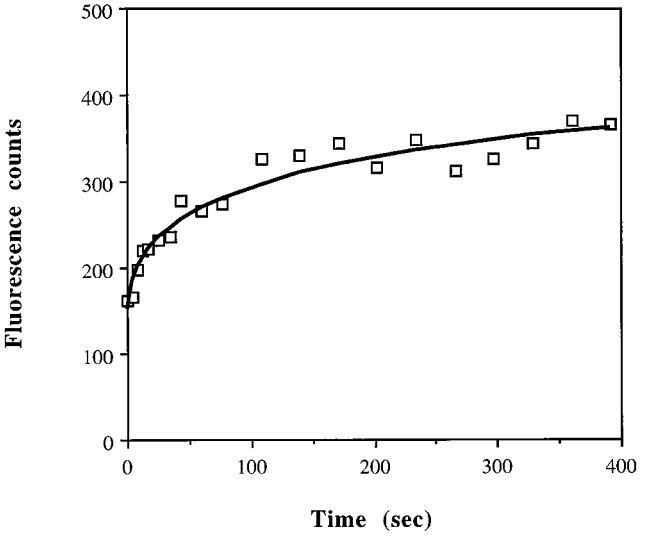

FIGURE 7 AQP1 FPR data fit to the anomalous subdiffusion model. Data from a representative AQP1 FPR experiment were reanalyzed using the anomalous subdiffusion model. This fit assumed 100% fractional mobility. The quality of the fit was comparable to that obtained using the standard random diffusion model (see Fig. 3).

indicates that all AQP1 molecules could be capable of lateral diffusion, but that the diffusion of these molecules is restricted by passive steric hindrance imposed by the dense membrane skeletal meshwork and/or by skeleton-linked membrane components.

As shown in Fig. 4, AQP1 redistribution after microdeformation does not resemble that of other integral proteins, including band 3 and glycophorin A. The AQP1 density gradient induced by microdeformation shows two distinctive features compared to the band 3 or glycophorin A gradients. First, the density gradient of AQP1 is less steep than those of band 3 and glycophorin A. Second, a substantial fraction (~50%) of AQP1 migrates toward the cap of the aspirated membrane projection. This behavior is similar to that of some membrane components that are not directly linked to the membrane skeleton, such as the lipid-linked membrane protein CD59 (Knowles et al., 1997). Together with the anomalous subdiffusion analysis (see above), these observations strongly suggest that AQP1 does not participate in direct binding interactions with the spectrin-based membrane skeleton, such as the band 3-ankyrin and glycophorin C-protein 4.1 interactions that serve to immobilize fractions of those integral proteins.

In conclusion, we note that the use of FPR and FIMD together to identify the physical constraints on AQP1 mobility has yielded a pattern of lateral mobility in the native membrane and redistribution in response to microdeformation that is thus far unique among integral membrane proteins. Future studies of this type may serve to extend these observations to other classes of membrane proteins that, like AQP1, are passively constrained by components associated with the dense (native) membrane skeleton, yet are able to diffuse rapidly in the plane of the membrane under conditions of skeletal "loosening" or removal.

We thank Dr. Bernie Thevenin for helpful discussions.

This work was supported by a Whitaker Foundation Biomedical Engineering Research Grant (MRC); and by National Institutes of Health grants HL 32854, HL 15157 (DEG); HL 33991, HL 48268, EY 11239 (PA); and HL 31579, DK 26263 (NM).

REFERENCES

Agre, P., G. M. Preston, B. L. Smith, J. S. Jung, S. Raina, C. Moon, W. B. Guggino, and S. Nielsen. 1993. Aquaporin CHIP: the archetypal molecular water channel. *Am. J. Physiol.* 265:F463–F476.

Axelrod, D., D. E. Koppel, J. Schlessinger, E. Elson, and W. W. Webb. 1976. Mobility measurements by analysis of fluorescence photobleaching recovery kinetics. *Biophys. J.* 16:1055–1069.

Bennett, V. 1983. Proteins involved in membrane-cytoskeleton association in human erythrocyte: spectrin, ankyrin, and band 3. *Methods Enzymol.* 96:313–324.

Berk, D. A., and R. M. Hochmuth. 1992. Lateral mobility of integral proteins in red blood cell tethers. *Biophys. J.* 61:9–18.

Bevington, P. R. 1969. Data Reduction and Error Analysis for the Physical Sciences. McGraw-Hill, New York.

Chasis, J. A., N. Mohandas, and S. Shohet. 1985. Erythrocyte membrane rigidity induced by glycophorin A-ligand interaction. Evidence for a ligand-induced association between glycophorin A and skeletal proteins. *J. Clin. Invest.* 75:1919–1926.

Chasis, J. A., M. Reid, R. Jensen, and N. Mohandas. 1988. Signal transduction by glycophorin A: role of extracellular and cytoplasmic domains in a modulatable process. *J. Cell Biol.* 107:1351–1357.

Cheng, A., A. van Hoek, M. Yeager, A. Verkman, and A. Mitra. 1997. Three-dimensional organization of a human water channel. *Nature.* 387:627–630.

Cho, M. R., S. W. Eber, S. E. Lux, and D. E. Golan. 1999. Regulation of band 3 rotational mobility by ankyrin in intact human red cells. *Biochemistry*. In press.

Corbett, J. D., P. Agre, J. Palek, and D. E. Golan. 1994a. Differential control of band 3 lateral and rotational mobility in intact red cells. *J. Clin. Invest.* 94:683–688.

Corbett, J. D., M. R. Cho, and D. E. Golan. 1994b. Deoxygenation affects fluorescence photobleaching recovery measurements of red cell membrane protein lateral mobility. *Biophys. J.* 66:25–30.

Corbett, J. D., and D. E. Golan. 1993. Band 3 and glycophorin are progressively aggregated in density-fractionated sickle and normal red blood cells. *J. Clin. Invest.* 91:208–217.

Denker, B. M., B. L. Smith, F. P. Kuhajda, and P. Agre. 1988. Identification, purification, and partial characterization of a novel M_r 28,000 integral membrane protein from erythrocytes and renal tubules. *J. Biol. Chem.* 263:15634–15642.

Discher, D. E., and N. Mohandas. 1996. Kinematics of red cell aspiration by fluorescence-imaged microdeformation. *Biophys. J.* 71:1680–1694.

Discher, D. E., N. Mohandas, and E. A. Evans. 1994. Molecular maps of red cell deformation: hidden elasticity and in situ connectivity. *Science.* 266:1032–1035.

Discher, D. E., R. Winardi, P. Schischmanoff, M. Parra, J. Conboy, and N. Mohandas. 1995. Mechanochemistry of protein 4.1's spectrin-actin-binding domain: ternary complex interactions, membrane binding, network integration, structural strengthening. *J. Cell Biol.* 130:897–907.

Ecelbarger, C., J. Terris, G. Frindt, M. Echevarria, D. Marples, S. Nielsen, and M. Knepper. 1995. Aquaporin-3 water channel localization and regulation in rat kidney. *Am J. Physiol.* 269:F663–F672.

Elkjaer, M., H. Birn, P. Agre, E. Christensen, and S. Nielsen. 1995. Effects of microtubule disruption on endocytosis, membrane recycling and polarized distribution of aquaporin-1 and gp330 in proximal tubule cells. *Eur. J. Cell Biol.* 67:57–72.

Feder, T. J., I. Brust-Mascher, J. P. Slattery, B. Baird, and W. W. Webb. 1996. Constrained diffusion or immobile fraction on cell surface: a new interpretation. *Biophys. J.* 70:2767–2773.

Frigeri, A., M. A. Gropper, F. Umenishi, M. Kawashima, D. Brown, and A. S. Verkman. 1995. Localization of MIWC and GLIP water channel homologs in neuromuscular, epithelial and glandular tissues. *J. Cell Sci.* 108:2993–3002.

Golan, D. E. 1989. Red blood cell membrane protein and lipid diffusion. *In* Red Cell Membrane. P. Agre and J. C. Parker, editors. Marcel Dekker, New York. 367–400.

Golan, D. E., M. R. Alecio, W. R. Veatch, and R. R. Rando. 1984. Lateral mobility of phospholipid and cholesterol in the human erythrocyte membrane: effects of protein-lipid interactions. *Biochemistry.* 23: 332–339.

Golan, D. E., J. D. Corbett, C. Korsgren, H. S. Thatte, S. Hayette, Y. Yawata, and C. M. Cohen. 1996. Control of band 3 lateral and rotational mobility by band 4.2 in intact erythrocytes: release of band 3 oligomers from low-affinity binding sites. *Biophys. J.* 70:1534–1542.

Golan, D. E., and W. Veatch. 1980. Lateral mobility of band 3 in the human erythrocyte membrane studied by fluorescence photobleaching recovery: evidence for control by cytoskeletal interactions. *Proc. Natl. Acad. Sci. USA.* 77:2537–2541.

Jarolim, P., H. L. Lubin, S. C. Liu, M. R. Cho, V. Brabec, L. H. Derick, S. J. Yi, S. T. Saad, S. Alper, C. Brugnara, D. E. Golan, and J. Palek. 1994. Duplication of 10 nucleotides in the erythroid band 3 (AE1) gene in a kindred with hereditary spherocytosis and band 3 protein deficiency. *J. Clin. Invest.* 93:121–130.

Jung, J. S., G. M. Preston, B. L. Smith, W. B. Guggino, and P. Agre. 1994. Molecular structure of the water channel through aquaporin CHIP: the hourglass model. *J. Biol. Chem.* 269:14648–14654.

Knowles, D. W., J. A. Chasis, E. A. Evans, and N. Mohandas. 1994. Cooperative action between band 3 and glycophorin A in human

erythrocytes: immobilization of band 3 induced by antibodies to glycophorin A. *Biophys. J.* 66:1726–1732.

Knowles, D. W., L. Tilley, N. Mohandas, and J. A. Chasis. 1997. Erythrocyte membrane vesiculation: model for the molecular mechanism of protein sorting. *Proc. Natl. Acad. Sci. USA.* 94:12969–12974.

Lacey, P. A., J. Robinson, M. L. Collins, D. G. Bailey, C. C. Evans, J. J. Moulds, and G. L. Daniels. 1987. Studies on the blood of a Co(a-b-) proposita and her family. *Transfusion.* 27:268–271.

Li, H., S. Lee, and B. Jap. 1997. Molecular design of aquaporin-1 water channel as revealed by electron crystallography. *Nature Struct. Biol.* 4:263–265.

Liu, S. C., J. Palek, S. J. Yi, P. E. Nichols, L. H. Derick, S. S. Chiou, D. Amato, J. D. Corbett, M. R. Cho, and D. E. Golan. 1995. Molecular basis of altered red cell membrane properties in Southeast Asian ovalocytosis: role of the mutant band 3 protein in band 3 oligomerization and retention by the membrane skeleton. *Blood.* 86:349–358.

Liu, S. C, S. Zhai, J. Palek, D. E. Golan, K. Amato, G. Hassan, T. Nurse, D. Babona, T. Coetzer, P. Jarolim, M. Zaik, and S. Borwein. 1990. Molecular defect of the band 3 protein in Southeast Asian ovalocytosis. *N. Engl. J. Med.* 323:1530–1538.

Lux, S. E., and J. Palek. 1995. Disorders of the red cell membrane. *In* Blood: Principles and Practice of Hematology. R. I. Handin, S. E. Lux, and T. P. Stossel, editors. J. B. Lippincott, Philadelphia. 1701–1818.

Marinelli, R., L. Pham, P. Agre, and N. LaRusso. 1997. Secretin promotes osmotic water transport in rat cholangiocytes by increasing aquaporin-1 water channels in plasma membrane. Evidence for a secretin-induced vesicular translocation of aquaporin-1. *J. Biol. Chem.* 272: 12984–12988.

Minton, A. P. 1989. Lateral diffusion of membrane proteins in protein-rich membranes: a simple hard particle model for concentration dependence of the two-dimensional diffusion coefficient. *Biophys. J.* 55:805–808.

Mohandas, N., and E. Evans. 1994. Mechanical properties of the red cell membrane in relation to molecular structure and genetic defects. *Annu. Rev. Biophys. Biomol. Struct.* 23:787–818.

Moulds, J. J., D. Mallory, and V. Zodin. 1978. Placental eluates: an economical source of antibodies. *Transfusion.* 18:388–389 (Abstr.).

Nash, G. B., and W. B. Gratzer. 1993. Structural determinants of the rigidity of the red cell membrane. *Biorheology.* 30:397–407.

Nielsen, S., L. King, B. Christensen, and P. Agre. 1997. Aquaporins in complex tissues. II. Subcellular distribution in respiratory and glandular tissues of rat. *Am. J. Physiol.* 273:C1549–C1561.

Nielsen, S., B. L. Smith, E. I. Christensen, M. A. Knepper, and P. Agre. 1993. Distribution of aquaporin CHIP in secretory and resorptive epithelia and capillary endothelia. *Proc. Natl. Acad. Sci. USA.* 90: 7275–7279.

Preston, G. M., B. L. Smith, M. L. Zeidel, J. J. Moulds, and P. Agre. 1994. Mutations in aquaporin-1 in phenotypically normal humans without functional CHIP water channels. *Science.* 265:1585–1587.

Rubin, H. 1963. Antibody elution from red blood cells. *J. Clin. Pathol.* 16:70–73.

Schnitzer, J. E., and P. Oh. 1996. Aquaporin-1 in plasma membrane and caveolae provides mercury-sensitive water channels across lung endothelium. *Am. J. Physiol.* 270:H416–H422.

Smith, B. L., and P. Agre. 1991. Erythrocyte M_r 28,000 transmembrane protein exists as a multi-subunit oligomer similar to channel proteins. *J. Biol. Chem.* 266:6407–6415.

Smith, B. L., G. M. Preston, F. A. Spring, D. J. Anstee, and P. Agre. 1994. Human red cell aquaporin CHIP. I. Molecular characterization of ABH and Colton blood group antigens. *J. Clin. Invest.* 94:1043–1049.

Stolpen, A., D. E. Golan, and J. S. Pober. 1988. Tumor necrosis factor and immune interferon act in concert to slow the lateral diffusion of proteins and lipids in human endothelial cell membranes. *J. Cell Biol.* 107: 781–789.

Terris, J., C. A. Ecelbarger, S. Nielsen, and M. A. Knepper. 1995. Long-term regulation of four renal aquaporins in rats. *Am. J. Physiol.* 271: F414–F422.

Walz, T., T. Hirai, K. Murata, J. Heymann, K. Mitsuoka, Y. Fujiyoshi, B. Smith, P. Agre, and A. Engel. 1997. The three-dimensional structure of aquaporin-1. *Nature.* 387:624–627.

Zeidel, M., S. Ambudkar, B. L. Smith, and P. Agre. 1992. Reconstitution of functional water channels in liposomes containing purified red cell CHIP28 protein. *Biochemistry.* 31:7436–7440.